RADPLEURA: A RADIOMICS-BASED FRAMEWORK FOR LUNG PLEURA CLASSIFICATION IN HISTOLOGY IMAGES FROM INTERSTITIAL LUNG DISEASES

Oscar Cuadros Linares[1,*]   *Ivar Vargas Belizario*[3]   *Sabrina Setembre Batah*[3]   *Bernd Hamann*[4]
Alexandre Todorovic Fabro [3]   *Paulo M. Azevedo-Marques*[3]   *Agma J. M. Traina*[2]

[1] Artificial Intelligence Lab., Recod.ai, Institute of Computing, University of Campinas (Unicamp), SP 13083-970, Brazil
[2]Institute of Mathematics and Computer Science (ICMC), University of Sao Paulo (USP), Sao Carlos, SP 13566-590, Brazil
[3]Faculty of Medicine, University of Sao Paulo, Ribeirao Preto, SP 14049-900, Brazil
[4]Department of Computer Science, University of California, Davis, CA 95616, U.S.A.

ABSTRACT

Lung pleura is a reference structure for the identification of histological characteristics for the recognition of a pathological interstitial lung disease (ILD) pattern. When a pattern is found, it is important to know whether it is close to the pleura to determine its specific type and severity. This manual process is tedious and laborious for the pathologist. Automating this task is important for a complete computed-system-assisted ILD diagnostic process. We introduce "RadPleura" a framework for pleura classification of histopathological images using a radiomics-based approach. Our framework performs image pre-processing, region-of-interest segmentation, and extraction of a radiomic-signature suited for ILD classification. To evaluate a radiomic-signature, we classify it into pleura and non-pleura, using two classifiers, a Support Vector Machine (SVM) and Gradient-boosted Decision Tree (GBD). Our experiments are promising, producing F-scores of 92% (SVM) and 91% (GBD). We also created a dataset of lung histopathology images with respective ground truth for pleura classification. To the best of our knowledge, this study is the first published attempt to explore and develop a radiomic signature for pleura classification. The methods have been integrated into the RadPleura framework developed.

Index Terms— Interstitial lung disease, Lung pleura, Histopathology, Radiomics, Machine learning

1. INTRODUCTION

Interstitial Lung Disease (ILD) belongs to a large group of different diseases related to architecture distortion and forms of pulmonary fibrosis [1]. The determination of histopathological patterns via Surgical Lung Biopsy (SLB) is crucial to reveal diagnostic clues. When specific patterns are found, it is important to measure their distance to the pleura. Thus, one routine task performed by pathologists is to identify the pleura

and determine its distance to the findings, as these measurements could indicate the disease stage and also help to classify it in a specific ILD etiology [2, 3]. We note that, differently from other medical imaging methods e.g., CT or MRI, there are no standard views (axial or coronal) for an SLB, which could support image analysis. Currently, there does not exist a single software tool or a method that aids specialists when analyzing an SLB for ILD diagnosis. Specialists must use many tools, for different parts of the analysis, such as ImageJ, QuPath, Cell Profiler, among others, that provide medical image processing algorithms, mainly for image pre-processing[4, 5, 6]. However, none of them aids when concerned with finding the lung pleura. Due to the lack of related work, we cannot provide a comparison against them.

Identifying the pleura serves as a reference to understand what is altered in the interstitium. The pleura is the unique region of the sampled tissue that does not move, i.e., it is always a boundary. Thus, the pleura region is the only guide for specialists. Fig. 1 shows an example of an SLB segment, showing pleural and non-pleural boundaries.
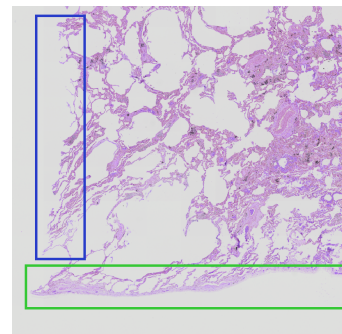
Fig. 1: Lung pleura in the green square and non-pleura in the blue square. Pleura boundaries are smoother and more regular than non-pleural boundaries.

To classify boundary regions as pleura or non-pleura, we introduce RadPleura, a radiomics-based approach using tex-

ture extractors for measuring the roughness heterogeneity of the pleura. The Radiomics approach was designed to maximize the extraction of high-dimensional features that include first-, second-, and higher-order statistics, from medical images. Radiomics was a method applied to find signatures in radiological data to understand tumor phenotypes [7]. Our goal was to establish a "radiomic signature" that captures the pleura heterogeneity in histopathology images. We included several Gray-Level Matrix (GLM) texture descriptors as well as those from Local Binary Patterns (LBPs). These measurements are well-known for accurately capturing roughness in surfaces [8] and texture in histology images [9]. We use these features to train two classifiers, a Support Vector Machine (SVM) and a Gradient-boosted Decision tree (GBD) to evaluate the classification properties of the radiomic signature. In addition, we developed a method for Region-of-Interest (ROI) segmentation, which includes a pre-processing step for noise elimination and background segmentation. We segment the ROI, defined as the external thick boundaries of each component in the sample, i.e., boundaries that separate the image background and the tissue. The main contributions of this work are listed below, summarizing the novelty of our proposed method:

- A fast and efficient ROI extraction for pleura detection
- A radiomic signature for pleura classification
- A dataset, with accurate ground truth, for lung pleura classification
- A web-based tool to aid in ILD diagnosis, includes our framework for pleura classification

2. FRAMEWORK

A summary of our framework for lung pleura classification is shown in Fig. 2.

2.1. Pre-processing

Histopathological images present problems, such as color irregularities due to staining procedures, irregular illumination, and many artifacts such as hand-made annotations, ink stains, and collage-like, straight lines due to the tile-staking process used in digitization. Fig. 2.1, shows examples of such problems.

To eliminate these problems, we apply a CIELab-based method to segment the tissue pixels (foreground) from all other elements, including noise and artifacts present in the images, and, at the same time to correct intensity-related issues. An important color-based feature of tissue, stained with Hematoxylin and Eosin, is the pink-scale intensity [10]. We can filter tissue pixels by selecting the pixels within the pink region in the CIELab color space, i.e., the pixels should be greater than zero for channel a and less than zero for channel b. Some noise may remain, nevertheless, most of the noise effects are filtered out, sufficiently for our application. All
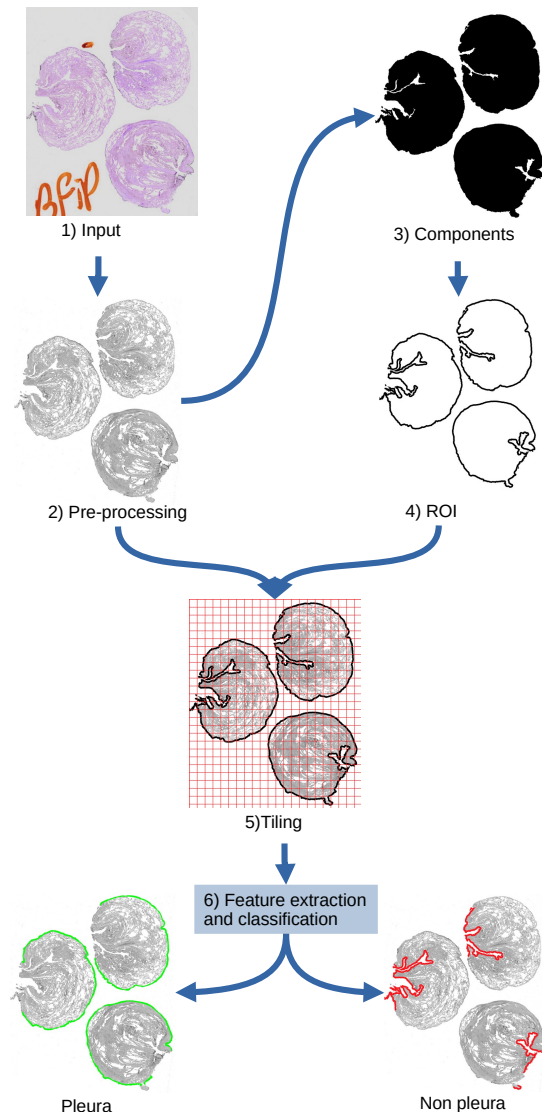
Fig. 2: RadPleura: (2.1) we first reduce noise and artifacts, improve contrast, and convert to gray-scale (2.2). Then, we identify the connected components (2.3), from which we segment the ROIs, i.e., thick boundaries (2.4). For feature extraction and classification, we divide the pre-processed image into isotropic tiles (2.5). We extract features from the ROIs (2.6). Finally, we classify feature vectors as pleura or non-pleura.

non-tissue pixels are replaced by a "white" pixel. After filtering out the non-desired pixels, we convert the CIELab image to a single RGB gray-scale image. Fig. 2.2 shows the generated output of this process.

2.2. Region-of-Interest Extraction

The Lung pleura is always located on the tissue boundary that we define as the ROI; it is a thick boundary, "a belt," of the tissue. Therefore, we detect only "external" boundaries, by first creating a binary version of the filtered image. This becomes

a simple task since all background pixels have been set to the same white color. We consider the image background as a single connected component so that we can confidently consider all non-background components to be part of the tissue region, even "holes" within the tissue. To segment the background as a single component, we apply a threshold-based region-growing algorithm (8-connected). We apply a padding process by one white pixel so that it connects possibly isolated background regions. This process is shown in Fig. 2.{2,3,4}. Next, we apply an algorithm to extract thick boundaries based on binary erosion, produces a small version of each component preserving the original shapes. Subsequently, by overlapping the original size components with the smaller ones after erosion, the non-overlapping region between them produces the expected thick boundary, shown in Fig. 2 4. We use this thick boundary as a binary mask to define the ROI. Feature extraction and pleura classification process can now be done.

2.3. Feature Extraction

To extract radiomic features we divide the image into isotropic non-overlapping tiles and extract feature vectors from the ROI segment in each tile. The LBP and GLM features are well-known "hand-crafted" texture descriptors with desirable properties, that, according to the concept of radiomics and when represented via a single 175-dimensional feature vector, should capture high-quality tissue information. We focus on texture descriptors since the lung pleura does not have a defined shape.

2.4. Classification and Feature Selection

We classify the feature vectors into two classes, pleura and non-pleura, using two classifiers, i.e., an SVM and a GBD. The goal of evaluating these classifiers is to evaluate their performance and better understand the radiomic signature of lung pleura for further improvements. Additionally, this is an important experiment since no related tool/system exists to build on or compare with.

On the other hand, features can be redundant, irrelevant, and/or linearly dependent. To select relevant features we apply a Sequential Floating Forward Search (SFFS) [11]. SFFS is a heuristic greedy algorithm commonly used for histology analysis [12] that adds features sequentially to increment the classification score.

3. EXPERIMENTS AND RESULTS

We have evaluated our method with histopathology images of human lungs SLB of subjects with a confirmed ILD. We have tested the radiomic signature with two classifiers, SVM and GBD. We have assessed each classifier with a) LBP; b) GLM; and c) LBP with GLM.

3.1. Histopathology Dataset

We created a dataset of 318 SLBs from subjects with confirmed ILD (from the Department of Pathology and Forensic Medicine, University of Sao Paulo, Ribeirao Preto, Brazil). The SLBs were digitized using a microscope power standardization of $20x$. We used an Olympus BX61 VS. microscope with pixel resolutions of $(110,019 \times 100,196)$ and $(128,018 \times 56,878)$, and physical isotropic pixel size of $(0.172\mu m \times 0.172\mu m)$. Each scanned slice was verified by three specialists.

To reduce sample size we re-scaled the dataset, from $20x$ to $1x$. We generated images of about $3k \times 3k$ pixel resolution, which is still large. However, at this lower resolution, we can apply our method in a practically acceptable time; about 20 seconds are needed on average for processing one image. We performed our experiments on a Linux workstation (Intel Core i7-2600 CPU 3.40GHz x 4 with 16GB memory).

The Ground Truth (GT) was manually created by physicians specialized in pulmonary pathology. The process of labeling consisted of painting the lung pleura using a brush tool[1]. This is a highly delicate task that must be done carefully, since many non-tissue (background) pixels can be wrongly labeled, even by an experienced specialist. Therefore, to improve the labeling, we only considered as lung pleura the painted tissue pixels and deleted painted background pixels. To perform this task, we "un-painted" the pixels outside the ROI using the method described in Section 2.2, producing the final GT image data. Our dataset along with the GT is freely available and can be downloaded, to encourage more research in lung pleura classification and computer-based histopathology analysis supporting ILD diagnosis. For more information, the corresponding author can be contacted.

3.2. Local Binary Patterns

We tested the SVM and GBD using LBP for different radii, ranging from 6 to 20, and a tile side size of 400 pixels. Radius values above 20 pixels are unsuitable for practical application due to the processing time required to extract the LBP patterns, about 125 seconds. The best F-score obtained using LBP was 0.87, for a radius value of 10. According to pathologists, this score is sufficient and acceptable for practical application.

3.3. Gray-level Texture Descriptors

We used the default parameter value settings suggested in [13] to evaluate the texture descriptors for compatibility with other published methods. We also evaluated the influence of tile side size, using values of 200, 300, 400, and 500 pixels. The F-scores for the SVM and GBD were 0.88 and 0.86, respectively, for a tile size of 500 pixels.

---

[1]GNU Image Manipulation Program (GIMP)

| (1) GT | (2) tile=200 | (3) P=0.87 NP=0.84 | (4) tile=500 | (5) P=0.96 NP=0.96 |
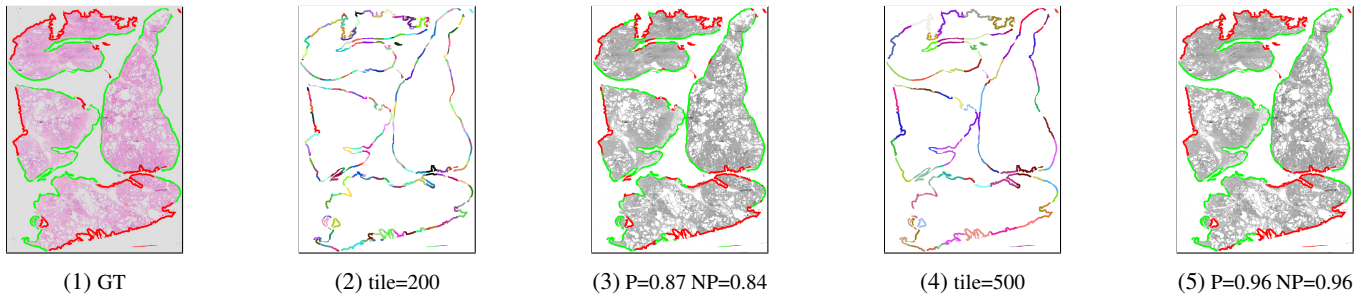
Fig. 3: Segmentation examples with corresponding DICE value. (1) Ground Truth (GT), pleural (P) regions in green and non-pleural (NP) regions in red; (2) colored visualization of ROIs for tile size 200 pixels; (3) SVM classification, pleural regions in green and non-pleural in red; (4) ROIs for tile size of 500 pixels; and (5) SVM.

3.4. LBP with GLM Features

We concatenated the LBP histograms and the GLM vectors, to define a single vector of 175 dimensions (82 LBP and 93 GLM dimensions). We analyzed the influence of tile size on the classification score. Table 1 shows the resulting values for F-score, precision and recall, using an LBP radius of 10 and isotropic tiles of side sizes 200, 300, 400, and 500 pixels, for the SVM and GBD classifiers. One sees that the combination of LBP and GLM features produced improved classification scores of 0.92 (SVM) and 0.91 (GBD).

classifier	tile	F-score	precision	recall
SVM	300	0.90	0.88	0.92
	400	0.91	0.89	0.92
	500	**0.92**	0.91	0.93
GDB	300	0.89	0.87	0.91
	400	0.90	0.88	0.91
	500	**0.91**	0.90	0.92

Table 1: F-score, precision, and recall values for SVM and GDB classifiers, using LBP and GLM features (10 k-fold).

3.5. Feature Selection

We used the Sequential Floating Forward Search (SFFS) Algorithm [11] to determine the number of selected features. The SVM algorithm was based on parameter values that produced the best results when using all features, i.e., radius value 10 and tile size 500. We sequentially applied the SFFS algorithm, reducing the number of features by five. The minimal number of selected features that ensures an F-score of at least 0.9 is 30.

3.6. Segmentation Quality Evaluation

In addition, we evaluated the segmentation quality for each image. We computed the DICE coefficient for pleura and non-pleura. The average coefficient values were 0.90 and 0.88, respectively. Fig. 3 shows two example results with the respective DICE coefficients.

3.7. Web Software Tool for ILD Diagnosis

We have developed a web-based tool that includes RadPleura, in addition to other methods like automatic cell-nuclei segmentation and ILD pattern ROI segmentation, see [14, 15]. It is available here: https://ivarvb.github.io/RadPleura/.

4. CONCLUSIONS

We have introduced a method for lung pleura classification in histopathological images. We employ the main steps of a machine learning approach: image pre-processing, background segmentation, ROI extraction, feature extraction, classification, and feature selection. The radiomics approach makes possible the extraction of many meaningful texture features to define a high-quality image signature. We used the feature vectors to evaluate two classifiers, SVM and GBD. The obtained F-score values of 92% demonstrate that a radiomics signature has the potential to characterize lung pleura for classification.

Furthermore, the obtained score is sufficient for practical application, i.e., the score suffices to guide pathologists in the analysis of biopsy samples. Our approach does not demand high-end computing platforms; it is possible to implement and use it on standard computers. Less than 20 seconds are needed for processing 500×500 tiles.

Concerning wrongly classified tiles, most of them are tiles with ROIs of very small size, containing limited information, most likely causing wrong classifications. Since we divide an image into a regular grid, some tiles may include small boundary regions. Another reason for wrong classification is the possibility that the sampling process (laboratory process) can cause pleural regions to lose their structure or get damaged. When these cases arise, they lead to "irregular training examples," and, consequently, classifiers do not learn how to classify such regions correctly. We intend to evaluate other classifiers, including deep-learning methods, in future work.

An important contribution of our research is the provision of the dataset for pleura classification. There is no cure for ILD; it is not possible to treat or heal damaged tissue. With our research and dataset, we hope to encourage more research to develop computer-based methods for ILD analysis.

5. REFERENCES

[1] William D Travis, Talmadge E King, Eric D Bateman, David A Lynch, Frédrique Capron, David Center, Thomas V Colby, Jean François Cordier, Roland M DuBois, Jeffrey Galvin, et al., "American thoracic society/european respiratory society international multidisciplinary consensus classification of the idiopathic interstitial pneumonias," *American journal of respiratory and critical care medicine*, vol. 165, no. 2, pp. 277–304, 2002.

[2] Rizwan A Qureshi, Tanveer A Ahmed, Antony D Grayson, Ajaib S Soorae, M John Drakeley, and Richard D Page, "Does lung biopsy help patients with interstitial lung disease?," *European journal of cardio-thoracic surgery*, vol. 21, no. 4, pp. 621–626, 2002.

[3] Y Li, Y Du, HF Yang, JH Yu, and XX Xu, "Ct-guided percutaneous core needle biopsy for small (≤ 20 mm) pulmonary lesions," *Clinical radiology*, vol. 68, no. 1, pp. e43–e48, 2013.

[4] Michael D Abràmoff, Paulo J Magalhães, and Sunanda J Ram, "Image processing with imagej," *Biophotonics international*, vol. 11, no. 7, pp. 36–42, 2004.

[5] Peter Bankhead, Maurice B Loughrey, José A Fernández, Yvonne Dombrowski, Darragh G McArt, Philip D Dunne, Stephen McQuaid, Ronan T Gray, Liam J Murray, Helen G Coleman, et al., "Qupath: Open source software for digital pathology image analysis," *Scientific reports*, vol. 7, no. 1, pp. 1–7, 2017.

[6] Michael R Lamprecht, David M Sabatini, and Anne E Carpenter, "Cellprofiler™: free, versatile software for automated biological image analysis," *Biotechniques*, vol. 42, no. 1, pp. 71–75, 2007.

[7] Hugo JWL Aerts, Emmanuel Rios Velazquez, Ralph TH Leijenaar, Chintan Parmar, Patrick Grossmann, Sara Carvalho, Johan Bussink, René Monshouwer, Benjamin Haibe-Kains, Derek Rietveld, et al., "Decoding tumour phenotype by noninvasive imaging using a quantitative radiomics approach," *Nature communications*, vol. 5, no. 1, pp. 1–9, 2014.

[8] A. Depeursinge, O.S. Al-Kadi, and J.R. Mitchell, *Biomedical Texture Analysis: Fundamentals, Tools and Challenges*, The MICCAI Society book Series. Elsevier Science, 2017.

[9] Meghana Dinesh Kumar, Morteza Babaie, Shujin Zhu, Shivam Kalra, and Hamid R Tizhoosh, "A comparative study of cnn, bovw and lbp for classification of histopathological images," in *2017 IEEE Symposium Series on Computational Intelligence (SSCI)*. IEEE, 2017, pp. 1–7.

[10] John KC Chan, "The wonderful colors of the hematoxylin–eosin stain in diagnostic surgical pathology," *International journal of surgical pathology*, vol. 22, no. 1, pp. 12–32, 2014.

[11] Pavel Pudil, Jana Novovičová, and Josef Kittler, "Floating search methods in feature selection," *Pattern recognition letters*, vol. 15, no. 11, pp. 1119–1125, 1994.

[12] Metin N Gurcan, Laura E Boucheron, Ali Can, Anant Madabhushi, Nasir M Rajpoot, and Bulent Yener, "Histopathological image analysis: A review," *IEEE reviews in biomedical engineering*, vol. 2, pp. 147–171, 2009.

[13] Joost JM Van Griethuysen, Andriy Fedorov, Chintan Parmar, Ahmed Hosny, Nicole Aucoin, Vivek Narayan, Regina GH Beets-Tan, Jean-Christophe Fillion-Robin, Steve Pieper, and Hugo JWL Aerts, "Computational radiomics system to decode the radiographic phenotype," *Cancer research*, vol. 77, no. 21, pp. e104–e107, 2017.

[14] Oscar Cuadros Linares, Bruno Faiçal, Paulo Barbosa, Bernd Hamann, Alexandre Fabro, and Agma Traina, "How to automatically identify regions of interest in high-resolution images of lung biopsy for interstitial fibrosis diagnosis," in *2019 IEEE 32nd International Symposium on Computer-Based Medical Systems (CBMS)*. IEEE, 2019, pp. 571–574.

[15] Oscar Cuadros Linares, Aurea Aurea Soriano-Vargas, Bruno S Faiçal, Bernd Hamann, Alexandre T Fabro, and Agma JM Traina, "Efficient segmentation of cell nuclei in histopathological images," in *2020 IEEE 33rd International Symposium on Computer-Based Medical Systems (CBMS)*. IEEE, 2020, pp. 47–52.